

# EFFICIENT MODELING OF LASER WAKEFIELD ACCELERATION THROUGH THE PIC CODE SMILEI IN CILEX PROJECT

Francesco Massimo\*, Arnaud Beck, Imen Zemzemi, Arnd Specka  
Laboratoire Leprince-Ringuet, 91128 Palaiseau, France

Julien Derouillat, Maison de la Simulation, 91191 Gif-sur-Yvette, France

Mickael Grech, Frédéric Pérez,

Laboratoire d'Utilisation des Lasers Intenses, 91128 Palaiseau Cedex, France

## Abstract

The design of plasma acceleration facilities requires considerable simulation effort for each part of the machine, from the plasma injector and/or accelerator stage(s), to the beam transport stage, from which the accelerated beams will be brought to the users or possibly to another plasma stage. The urgent issues and challenges in simulation of multi-stage acceleration with the Apollon laser of CILEX facility will be addressed. To simulate the beam injection in the second plasma stage, additional physical models have been introduced and tested in the open source Particle in Cell collaborative code SMILEI. The efficient initialisation of arbitrary relativistic particle beam distributions through a Python interface allowing code coupling and the self consistent initialisation of their electromagnetic fields will be presented. The comparison between a full PIC simulation and a simulation with a recently developed envelope model, which allows to drastically reduce the computational time, will be also shown for a test case of laser wakefield acceleration of an externally injected electron beam.

## INTRODUCTION

Laser Wakefield Acceleration (LWFA) is a promising technique to accelerate particles with gradients order of magnitudes higher than those of metallic accelerating cavities [1–3]. A high intensity laser pulse propagating in a plasma and of length of the order of the plasma wavelength can create a cavity empty of electrons in its wake. In this “bubble”, the generated high gradient wakefields are suitable for electron focusing and acceleration. The realization of the PetaWatt laser Apollon in the CILEX (Centre Interdisciplinaire Lumière EXtrême) facility [4] in France will pave the way to innovative LWFA experiments. The use of a second plasma stage of LWFA in the weakly nonlinear regime is considered, implying both experimental and modelization challenges. In this work we present new features in the Particle-in-Cell (PIC) code SMILEI [5] to address the simulation challenges of the project.

The length of the first plasma stage, acting as an electron injector in nonlinear regimes, is of the order of millimeters. The length of this second stage will instead need to be at least of the order of the centimeters in order to accelerate particles at high energies with the less intense fields generated in weakly nonlinear regimes. The standard PIC

technique [6] would be unfeasible for the much longer distances to simulate required by the second plasma stage. A solution to considerably reduce the computation time consists in using an envelope model for the laser pulse [7, 8]. In this approach one only needs to sample the envelope spatio-temporal scales, of the order of the plasma wavelength  $\lambda_p$  and frequency  $\omega_p = 2\pi c/\lambda_p = c/k_p$  instead of the laser wavelength  $\lambda_0$  and frequency  $\omega_0 = 2\pi c/\lambda_0$ . Doing so allows for a coarser, and cheaper, resolution while retaining all the relevant physics. The use of cylindrical symmetry in an envelope model, like in [9] would be unsuited for CILEX, since even a cylindrically symmetric beams exiting from the first plasma stage would be influenced by the intrinsic asymmetry in the focusing elements of the conventional transport line towards the second plasma stage. Thus, we developed a 3D completely parallelized envelope model for the laser-plasma dynamics, first implemented in the PIC code ALaDyn [10] and described in detail in [8]. In this paper, we briefly recall the envelope model's equations and the initialization of arbitrary beam phase distributions with their self-consistent electromagnetic fields, as initial conditions for a simulation (following the procedure described in [11, 12]). Both these features have been implemented in SMILEI. After showing the results of two validation tests of the envelope model against analytical theory, we show an application of these two features in a SMILEI simulation of a second plasma stage of LWFA.

## ENVELOPE MODEL

The hypothesis of the envelope model, i.e. a shape of the laser pulse vector potential  $\mathbf{A}$  given by a slowly varying complex envelope  $\tilde{\mathbf{A}}$  modulated by oscillations at the laser frequency  $\omega_0 = k_0 c$  can be expressed as

$$A(\mathbf{x}, t) = \text{Re}[\tilde{A} e^{ik_0(x-ct)}]. \quad (1)$$

The laser pulse is supposed to propagate in the positive  $x$  direction. Following [8], the envelope hypothesis can be inserted in D'Alembert's Equation for the laser vector potential, obtaining the envelope equation in laboratory coordinates, solved in [8] and in SMILEI:

$$\nabla \tilde{A} + 2ik_0 \left( \partial_x \tilde{A} + \frac{1}{c} \partial_t \tilde{A} \right) - \frac{1}{c^2} \partial_t^2 \tilde{A} = \chi \tilde{A}, \quad (2)$$

where  $\chi$  is the plasma susceptibility, which takes into account the envelope modification due to the presence of the

\* massimo@lir.in2p3.fr

plasma. The susceptibility term is computed as

$$\chi = \sum_p^{N_{\text{particles}}} \frac{q_p^2}{c^2 \epsilon_0 m_p} \frac{n_p}{\bar{\gamma}_p}. \quad (3)$$

where  $q_p$ ,  $m_p$ ,  $\bar{n}_p$ ,  $\bar{\mathbf{p}}_p$  and  $\bar{\gamma}_p$  are respectively the particle  $p$ 's charge, mass, number density, momentum and ponderomotive Lorentz factor, defined as

$$\bar{\gamma}_p = \sqrt{1 + \frac{\|\bar{\mathbf{p}}_p\|^2}{m_p^2 c^2} + \frac{q_p^2}{m_p^2 c^2} \frac{\|\bar{\tilde{A}}(\bar{\mathbf{x}}_p)\|^2}{2}}, \quad (4)$$

where  $\bar{\mathbf{x}}_p$  is the particle  $p$ 's position. The bar over the physical quantities above refers to the fact that they are averaged over the optical cycle. The same notation will be used in the following.

The electromagnetic fields  $\bar{\mathbf{E}}$ ,  $\bar{\mathbf{B}}$  evolve according to the averaged Maxwell's equations:

$$\begin{aligned} \partial_t \bar{\mathbf{B}} &= -\nabla \times \bar{\mathbf{E}} \\ \partial_t \bar{\mathbf{E}} &= c^2 \nabla \times \bar{\mathbf{E}} - c^2 \mu_0 \bar{\mathbf{J}}. \end{aligned} \quad (5)$$

As result of the averaging process [7], the particles averaged equations of motion contain the ponderomotive force term in the momentum equation and become

$$\begin{aligned} \frac{d\bar{\mathbf{x}}_p}{dt} &= \frac{\bar{\mathbf{p}}}{m_p \bar{\gamma}_p} \\ \frac{d\bar{\mathbf{p}}_p}{dt} &= q_p \left[ \bar{\mathbf{E}}(\bar{\mathbf{x}}_p) + \frac{\bar{\mathbf{p}}_p}{m_p \bar{\gamma}_p} \times \bar{\mathbf{B}}(\bar{\mathbf{x}}_p) \right] + \\ &- \frac{q_p^2}{4m_p \bar{\gamma}_p} \nabla \|\bar{\tilde{A}}\|^2(\bar{\mathbf{x}}_p). \end{aligned} \quad (6)$$

As described in [8], the envelope equation Eq. (2) can be discretized through centered finite differences, obtaining an explicit solver scheme which is easily parallelizable. Maxwell's equations Eq. (5) are solved as in standard PIC codes or with more advanced dispersion-free schemes [5, 6], while the particles equations of motion are solved using a modified Boris pusher scheme, described in [8]. Some equations of the envelope model, as the momentum evolution equation Eq. (7) contain the ponderomotive Lorentz factor  $\bar{\gamma}$ , which depends on the envelope  $\bar{A}$  itself. The standard PIC temporal loop [6] must be modified to solve the above equations with the schemes described in [8]. The modified temporal loop of Smilei in envelope mode is shown in Fig. 1. At each time iteration, the electromagnetic force (including the ponderomotive force) acting on each particle is interpolated from the grid. The susceptibility of each particle is then projected on the grid, following Eq. (3). The particles momenta are updated through the use of the force they are subject to, solving Eq. (7) through a modified Boris pusher described in [8]. The envelope equation is then solved, advancing the envelope value in time. The explicit envelope solver scheme is described in detail in [8]. The particles positions are updated solving Eq. (6) as described in [8].

The particles current density is projected then on the grid and the electromagnetic fields are advanced through a Yee scheme [6]. The loop iteration can then be repeated until the end of the simulation.

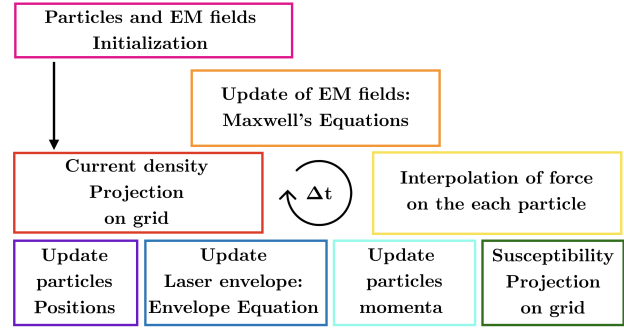


Figure 1: The envelope PIC temporal loop, showing the operations performed at each temporal iteration.

## RELATIVISTIC BEAM INITIALIZATION

Under the hypothesis of monoenergetic phase space distribution, the electromagnetic fields of a relativistic particle beam can be initialized in a simulation through the technique explained in [11, 12], here briefly recalled. This technique has been implemented in SMILEI to perform simulations of LWFA with external injection of an electron beam into a second plasma stage. Once the beam charge density  $\bar{\rho}$  is known, the “relativistic Poisson's equation”, i.e.

$$\left( \frac{1}{\gamma_0^2} \partial_x^2 + \nabla_\perp^2 \right) \bar{\Phi} = -\frac{\bar{\rho}}{\epsilon_0}, \quad (8)$$

gives  $\bar{\Phi}$  and the beam self-consistent electromagnetic fields can be found through the relations:

$$\bar{\mathbf{E}} = \left( -\frac{1}{\gamma_0^2} \partial_x, -\partial_y, -\partial_z \right) \bar{\Phi} \quad (9)$$

$$\bar{\mathbf{B}} = \beta_0 c \hat{x} \times \bar{\mathbf{E}}. \quad (10)$$

SMILEI allows to easily define an initial beam distribution through its Python input interface, which permits to define ideal bunches as well as load datafiles with beam distributions obtained from transport codes.

## ENVELOPE MODEL BENCHMARKS AGAINST ANALYTICAL THEORY

As first tests for the envelope model feature of SMILEI, this section presents the simulation of vacuum diffraction of a Gaussian laser beam and of the laser wakefield inside a plasma in the linear regime. Figure 2 reports the comparison between the simulated rms waist size of a Gaussian beam with initial waist  $w_0 = 12 \mu\text{m}$  and the vacuum Rayleigh diffraction formula  $w(\bar{x})/w_0 = \sqrt{1 + \bar{x}^2}$ , where  $\bar{x} = x/Z_R$  is the propagation distance divided by the Rayleigh length

$Z_R = \pi w_0^2 / \lambda_0$  [13]. The longitudinal grid cell size, the transverse grid cell size and the timestep are respectively  $\Delta x = 0.69 c / \omega_0$ ,  $\Delta y = \Delta z = 5 c / \omega_0$ ,  $\Delta t = 0.57 1 / \omega_0$ .

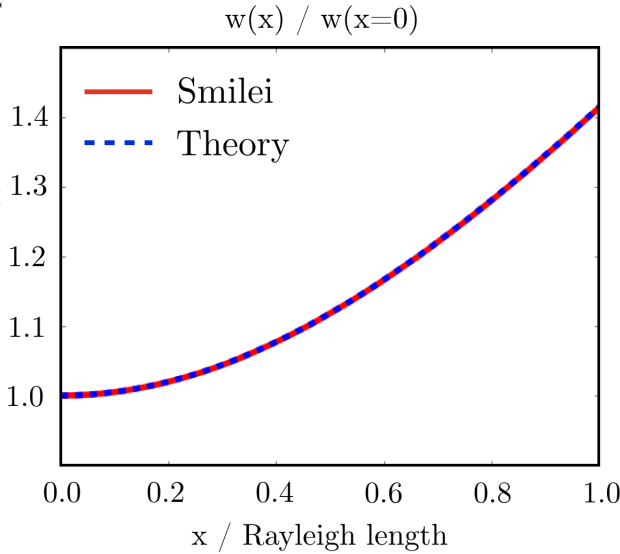


Figure 2: Evolution of the waist size  $w(x)$  of a Gaussian laser pulse simulated through the envelope model against analytical theory.

The second validation test we report (see Fig. 3) is a comparison of the results of the envelope model against the analytical theory for the longitudinal wakefield  $E_x$  of a Gaussian laser pulse in a plasma in the linear regime (Eq. (37a) from [14]):

$$E_x(x, r, t) = \frac{mc^2 k_p^2}{e} \frac{1}{4} \int_z^\infty a(x', r, t) e^{-\frac{r^2}{w_0^2}} \cos[k_p(x-x')] dx', \quad (11)$$

for a laser pulse with envelope  $A(x, r, t) = a(x, t) e^{-r^2/w_0^2}$  and  $w_0 \gg \lambda_p$ . For this benchmark, we chose an initial waist size of  $12 \mu\text{m}$  and a Gaussian longitudinal envelope  $a(x, t = 0)$  with initial FWHM duration in intensity  $\tau_0 = 20$  fs and peak value  $a_0 = 0.01$ , to remain in a linear regime. The plasma density is  $n_0 = 0.0017 n_c$ . The same grid cell size and timesteps as the vacuum diffraction benchmark have been used, and 8 particles per cell sample the plasma.

For both the benchmarks, we observe a very good agreement with the analytical predictions.

## CASE STUDY: EXTERNAL INJECTION IN A SECOND PLASMA STAGE

As a benchmark and as an example of application of both the envelope model and the relativistic beam field initialization, we present the preliminary results of two simulations, one performed with a standard PIC procedure (hereafter called “standard laser simulation”) and one with an envelope model for the laser (hereafter called “envelope simulation”). The physical setup is the external injection of a relativistic electron beam (whose fields have been initialized with the procedure described above) into the plasma wave in the wake

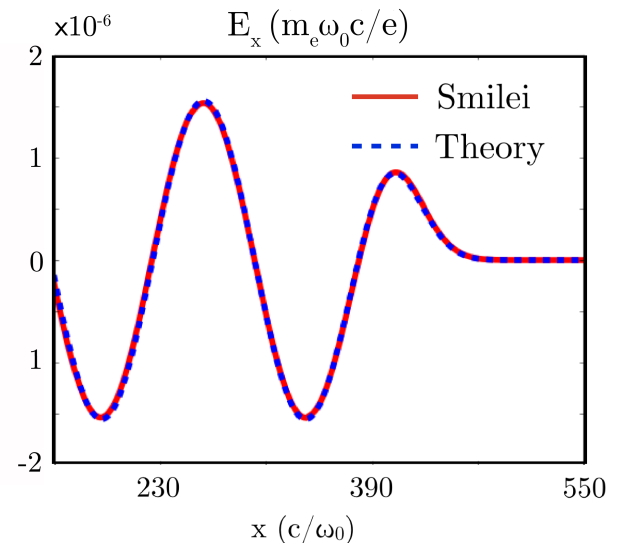


Figure 3: Simulated longitudinal electric field in the wake of a Gaussian laser pulse modeled through the envelope against the analytical linear theory. The laser is propagating towards right.

of a laser in a plasma stage. The laser, plasma and electron beam parameters, briefly recalled in the following, have been chosen from [15]. The driver laser is a Gaussian pulse, linearly polarized in the  $y$  direction, with waist size  $w_0 = 45 \mu\text{m}$ ,  $a_0 = \sqrt{2}$  and initial FWHM duration in intensity  $\tau_0 = 108$  fs, focused at the plasma entrance. The initial laser center position is at a distance  $2c\tau_0$  from the plasma entrance. The plasma has an idealized parabolic density profile along the transverse direction with density  $n_e(r) = n_0 \left(1 + \frac{\Delta n}{n_0} \frac{r^2}{r_0^2}\right)$ , with  $r$  the distance to axis,  $n_0 = 1.5 \cdot 10^{17} \text{cm}^{-3}$ ,  $\frac{\Delta n}{n_0} = 0.25$ ,  $r_0 = 45 \mu\text{m}$ . The relativistic electron beam, with charge  $30 \text{pC}$  and normalized emittance  $1 \text{mm}\cdot\text{mrad}$ , has an initial energy of  $150 \text{MeV}$  with  $0.5\%$  rms energy spread and is initially positioned at waist at a distance  $3/4\lambda_p$  after the laser pulse. The beam longitudinal and transverse rms sizes are  $\sigma_x = 2 \mu\text{m}$  and  $\sigma_y = \sigma_z = 1.3 \mu\text{m}$ . The grid cell sizes for the standard laser simulation are  $\Delta x_{\text{laser}} = \lambda_0/32$ ,  $\Delta y = \Delta z = \lambda_0$  and the integration timestep is  $\Delta t_{\text{laser}} = 0.95\Delta x/c$ . For the envelope simulation, because the length of the laser pulse envelope is so much longer than a single optical cycle, the longitudinal grid cell size and the integration timestep could be set to  $\Delta x_{\text{envelope}} = 16\Delta x_{\text{laser}}$ ,  $\Delta t_{\text{envelope}} = 0.8\Delta x_{\text{envelope}}$  respectively. The transverse cell length is the same as in the standard laser simulation. In both simulations, the plasma is sampled with 8 particles per cell and the beam is sampled with  $10^6$  particles. Figures 4 and 5 compare the colormaps of the electron density  $n_e$  and of the longitudinal electric field  $E_x$  for the two simulations after a propagation distance of  $3 \text{mm}$  in the plasma. Figures 6 and 7 compare the same quantities on the axis at the same propagation distance. Apart from a minimum lag of the electron beam behind the laser pulse in the case of the envelope simulation, the results have a very good agreement. The envelope simulation reproduces

the laser and plasma dynamics, as well as the beam loading of the bunch on the plasma wave. Further investigations are necessary to understand the differences in the dynamics of the electron beam in the two simulations. The greater dilution of the electron beam in the envelope simulation may be caused by a different growth rate of the numerical Cherenkov radiation [16], due to the difference mesh cell size and integration timestep compared to the standard laser simulation. The envelope simulation needed 4400 CPU hours, while the standard laser simulation needed a total amount of resources twenty times as large.

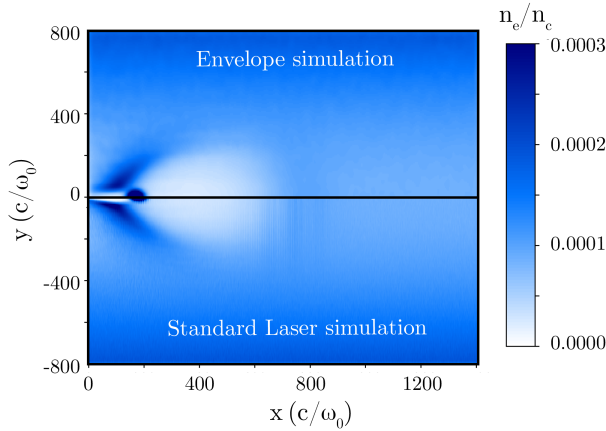


Figure 4: Electron charge density, normalized by the critical density  $n_c$ , after 3 mm of propagation in the plasma.

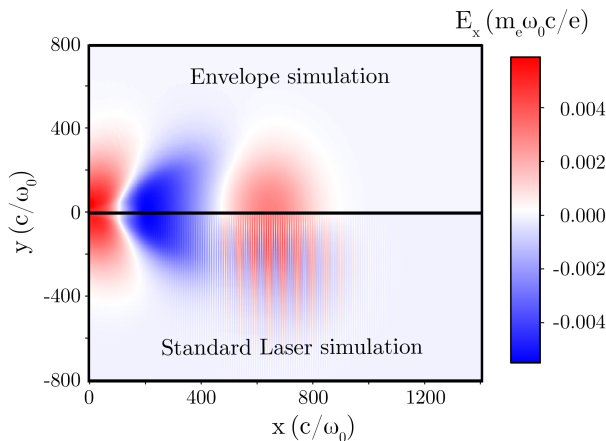


Figure 5: Longitudinal electric field  $E_x$  after 3 mm of propagation in the plasma.

## CONCLUSIONS

A 3D explicit envelope model and a procedure for the initialization of relativistic particle beams electromagnetic fields have been implemented in the PIC code SMILEI. These techniques have been developed to face the modelization challenges of the multi-stage LWFA experiments in the CILEX project. We reported the results benchmarks of the

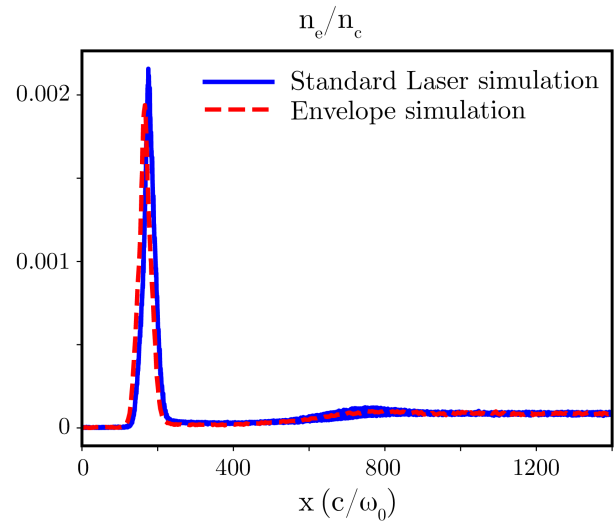


Figure 6: Electron charge density on the propagation axis, normalized by the critical density  $n_c$ , after 3 mm of propagation in the plasma.

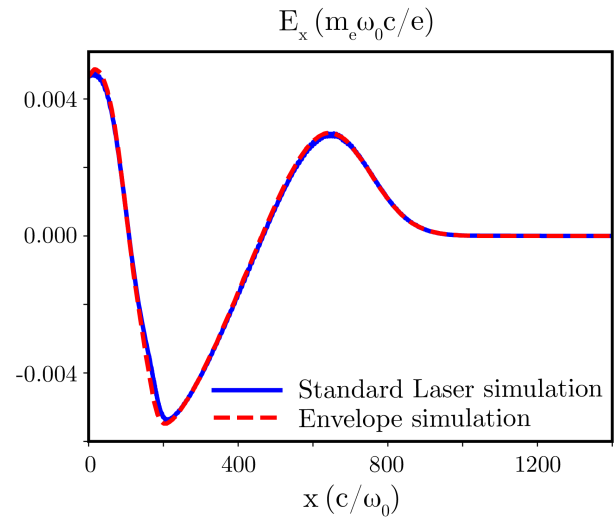


Figure 7: Longitudinal electric field  $E_x$  on the propagation axis after 3 mm of propagation in the plasma.

envelope model against analytical theory for laser vacuum diffraction and linear laser wakefield in the plasma. We presented also the comparison between a standard 3D PIC simulation and a 3D PIC simulation with envelope model for the laser in the case of external injection of an electron beam in a plasma channel. Excellent agreement is found after 3 mm of propagation, with a computational speedup of 20 using the envelope model.

## ACKNOWLEDGEMENTS

The project has received funding from the P2IO LabEx (ANR-10-LABX-0038) in the framework “Investissements d’Avenir” (ANR-11-IDEX-0003-01) managed by the Agence Nationale de la Recherche (ANR, France). This work was granted access to the HPC resources of TGCC/CINES un-

der the allocation 2018-A0030510062 and Grand Challenge “Irene” 2018 project gch0313 made by GENCI. The authors are grateful to the TGCC and CINES engineers for their support. The authors thank engineers of the LLR HPC clusters for resources and help. The authors are grateful to the ALaDyn development team for the help and discussions during the development of the envelope model, in particular D. Terzani, A. Marocchino and S. Sinigardi.

## REFERENCES

- [1] T. Tajima, J.M. Dawson, *Phys. Rev. Lett.* 43 (4), 1979, p. 267.
- [2] E. Esarey, C. B. Schroeder, W. P. Leemans, *Rev. Mod. Phys.* 81, 2009, p. 1229.
- [3] V. Malka, *Phys. Plasmas* 19, 2012, p. 055501.
- [4] B. Cros et al., *Nucl. Instr. and Meth. in Phys. A* 740, 2014, p. 27.
- [5] J. Derouillat, A. Beck, F. Pérez, T. Vinci, M. Chiaramello, A. Grassi, M. Flé, G. Bouchard, I. Plotnikov, N. Aunai, J. Dargent, C. Riconda, M. Grech, *Comput. Phys. Comm.* 222, 2018, p. 351.
- [6] C. K. Birdsall, A. B. Langdon, *Plasma Physics Via Computer Simulation* CRC Press, Boca Raton, 2004.
- [7] B.M. Cowan, D.L. Bruhwiler, E. Cormier-Michel, E. Esarey, C.G.R. Geddes, P. Messmer, K. M. Paul, *Journal of Computational Physics* 230, 2011, p. 61.
- [8] D. Terzani, P. Londrillo, “Yet a faster numerical implementation of envelope model for laser-plasma dynamics,” submitted to *Computer Physics Communications*.
- [9] C. Benedetti, E. Esarey, W. P. Leemans, C. B. Schroeder, in *Proc. ICAP 2012*, 2012.
- [10] S. Sinigardi, A. Marocchino, P. Londrillo, D. Terzani, F. Massimo, F. Mira, A. Sgattoni, *ALaDyn/ALaDyn: ALaDyn v2018.2 (Version v2.1.0)*. Zenodo, 2018, <http://doi.org/10.5281/zenodo.1406920>.
- [11] F. Massimo, A. Marocchino, A.R. Rossi, *Nucl. Instrum. Meth. A* 829, 2016, p. 378.
- [12] J.-L. Vay, *Phys. Plasmas* 15, 2008, p. 056701.
- [13] O. Svelto, *Principles of Lasers* Springer US, 2012.
- [14] R. Lehe, M. Kirchen and I. A. Andriyash, B. B. Godfrey, J.-L. Vay, *Comput. Phys. Comm.* 203, 2015, p. 66.
- [15] X. Li, A. Mosnier, P. A. P. Nghiem, “Design of a 5 GeV laser plasma accelerating module in the quasi-linear regime”, *Nucl. Instrum. Meth. A*, in press, 2018.
- [16] R. Lehe, A. Lifschitz, C. Thauray, V. Malka, X. Davoine, *Phys. Review Special Topics Acc. and Beams* 16, 2013, p. 021301.